

First-principles calculation of band offsets, optical bowings, and defects in CdS, CdSe, CdTe, and their alloys

Su-Huai Wei, S. B. Zhang, and Alex Zunger

Citation: *Journal of Applied Physics* **87**, 1304 (2000); doi: 10.1063/1.372014

View online: <http://dx.doi.org/10.1063/1.372014>

View Table of Contents: <http://scitation.aip.org/content/aip/journal/jap/87/3?ver=pdfcov>

Published by the [AIP Publishing](#)

Articles you may be interested in

[Band structure measurement and analysis of the Bi₂Te₃/CdTe \(111\)B heterojunction](#)

J. Vac. Sci. Technol. A **33**, 031602 (2015); 10.1116/1.4914175

[Predicted roles of defects on band offsets and energetics at CIGS \(Cu\(In,Ga\)Se₂/CdS\) solar cell interfaces and implications for improving performance](#)

J. Chem. Phys. **141**, 094701 (2014); 10.1063/1.4893985

[First-principles study of valence band offsets at ZnSnP₂/CdS, ZnSnP₂/ZnS, and related chalcopyrite/zincblende heterointerfaces](#)

J. Appl. Phys. **114**, 043718 (2013); 10.1063/1.4816784

[Valence band offset at the CdS/CdTe interface](#)

J. Vac. Sci. Technol. B **20**, 1777 (2002); 10.1116/1.1491989

[Measurements and calculations of the valence band offsets of SiO_x / ZnS \(111\) and SiO_x / CdTe \(111\) heterojunctions](#)

J. Vac. Sci. Technol. B **16**, 989 (1998); 10.1116/1.590056



Frustrated by old technology? Is your AFM dead and can't be repaired? Sick of bad customer support?

It is time to upgrade your AFM

Minimum \$20,000 trade-in discount for purchases before August 31st

Asylum Research is today's technology leader in AFM

dropmyoldAFM@oxinst.com

OXFORD INSTRUMENTS
The Business of Science®

First-principles calculation of band offsets, optical bowings, and defects in CdS, CdSe, CdTe, and their alloys

Su-Huai Wei^{a)}, S. B. Zhang, and Alex Zunger
National Renewable Energy Laboratory, Golden, Colorado 80401

(Received 16 August 1999; accepted for publication 18 October 1999)

Using first principles band structure theory we have calculated (i) the alloy bowing coefficients, (ii) the alloy mixing enthalpies, and (iii) the interfacial valence band offsets for three Cd-based (CdS, CdSe, CdTe) compounds. We have also calculated defect formation energies and defect transition energy levels of Cd vacancy V_{Cd} and Cu_{Cd} substitutional defect in CdS and CdTe, as well as the isovalent defect Te_S in CdS. The calculated results are compared with available experimental data.

© 2000 American Institute of Physics. [S0021-8979(00)01103-8]

I. INTRODUCTION

Cd-based II-VI semiconductor compounds and alloys have attracted considerable interest in the last few years due to their applications in photovoltaic devices.^{1,2} CdTe has an ideal band gap and high absorption coefficient which makes it one of the strong contenders for low cost, high efficiency thin-film solar cell materials, having achieved efficiency in excess of³ 15%. CdS is also widely used as an *n*-type window material in thin-film solar cell devices. However, many fundamental physical properties of the Cd-based semiconductor systems are not well understood. For examples, the formation of the CdTe/CdS interface is accompanied by an interdiffusion of Te in CdS or vice versa,⁴ creating $CdS_{1-x}Te_x$ alloy. It is not clear (i) how the band gap and the band edge states vary as a function of the alloy composition *x*. (ii) What causes a large band gap reduction in the CdS layer (leading to lower quantum efficiency⁵) when small amounts of Te are present. (iii) Why photogenerated holes in CdS are not contributing to the photocurrent.⁶ (iv) Why Cu doping in CdTe induces (*p*-type) conductivity, while Cu doping in CdS produce only high resistivity samples. There are also a number of theoretical questions of interest here.

(a) *The effect of cation *d* states on valence band offsets.*⁷ It is known that cation *d* and anion *p* coupling reduces the band offsets in II-VI compounds.⁸ The *p*–*d* coupling increases with small *p*–*d* energy differences and large overlap between the *p*–*d* orbitals. Comparing Zn with Cd, one notes that Zn has higher *d* orbital energy and smaller atomic size, suggesting larger *p*–*d* coupling. However, the 3*d* orbital of Zn is more localized than Cd, suggesting smaller *p*–*d* coupling. It will, therefore, be interesting to find out whether Zn compounds or Cd compounds has larger *p*–*d* coupling, thus larger band offsets.

(b) *The doping limit rule.*⁹ It has been shown that the formation energies at a fixed absolute Fermi energy are approximately the same for close-shell defects [e.g., V_{Ga}^{3-} in GaX (X=N, P, As, Sb)] in all III-V materials.¹⁰ At a critical Fermi energy, the formation energy of the close-shell defects changes from positive to negative. Since doping moves the

Fermi energy, the spontaneous formation of compensating defect will prevent further doping, thus the shift of the Fermi energy. It will be interesting to see whether this rule applies also to II-VI compounds (e.g., Cd vacancy V_{Cd} in Cd compounds).

(c) *The vacuum pinning rule.* It has also been shown that the electrical transition energy levels of a given deep level impurity (e.g., Fe in II-VI compounds) tend to line-up relative to vacuum level.¹¹ It will be interesting to see whether this effect holds for impurities whose wave functions are less localized (e.g., Cu substitutional defect Cu_{Cd} in Cd compounds).

To answer these questions, we have studied systematically the electronic structures of Cd-based compounds, alloys, interfaces and Cu_{Cd} and V_{Cd} impurities in Cd compounds using the first-principles, self-consistent electronic structure theory based on the local density approximation¹² (LDA). We calculated (a) the alloy mixing enthalpy ΔH at *x*=1/2, (b) the heterojunction valence band offset ΔE_v , (c) the alloy band gap bowing parameters *b*, (d) the energy levels of the isovalent defects of Te and Te-Te pair substitution in CdS, and (e) the formation energies and the transition energy levels of Cu_{Cd} and V_{Cd} in CdS and CdTe. This article describes how such calculations are done and discusses the significant physics of the results.

II. METHOD OF CALCULATION

The band structure and total energy calculations are performed using the first-principles density functional formalism as implemented by the general potential, all electron, relativistic, linearized augmented plane wave (LAPW) method.¹³ The Cd *d* electrons are treated in the same footing as the other valence states. No shape approximations are employed for either the potential or the charge density. We used the Ceperley-Alder exchange correlation potential¹⁴ as parameterized by Perdew and Zunger.¹⁵ The Brillouin zone integration of the superstructures is performed using special *k* points which are equivalent¹⁶ to the 10 special *k* points in the zinc-blende Brillouin zone. We assume the zinc-blende crystal structure, although the stable crystal structure of CdS are wurtzite. We use the experimental lattice constants¹⁷ *a*

^{a)}Electronic mail: swei@nrel.gov

=5.818, 6.052, and 6.482 Å for CdS, CdSe, and CdTe, respectively, for electronic structure calculations. The LDA calculated lattice constants¹⁸ are within 0.7% of the experimental values.

A. Band offsets

To calculate the valence band offset $\Delta E_v(\text{CdX}/\text{CdY})$ at the interface between two Cd compounds CdX and CdY we follow the procedure^{7,8} used in photoemission core-level spectroscopy, where the band offset is given by

$$\Delta E_v(\text{CdX}/\text{CdY}) = \Delta E_{\text{VBM},\text{C}}^{\text{CdX}} - \Delta E_{\text{VBM}',\text{C}'}^{\text{CdY}} + \Delta E_{\text{C},\text{C}'}. \quad (1)$$

Here, $\Delta E_{\text{VBM},\text{C}}^{\text{CdX}} = E_{\text{VBM}}^{\text{CdX}} - E_{\text{C}}^{\text{CdX}}$ is the core level to valence band maximum energy separations for CdX and $\Delta E_{\text{C},\text{C}'} = E_{\text{C}}^{\text{CdX}} - E_{\text{C}'}^{\text{CdY}}$ is the difference in core level binding energy between CdX and CdY on each side of the interface. To obtain the unstrained (natural) band offset, the first two terms in Eq. (1) are calculated at their respective equilibrium structural parameters appropriate to the isolated compounds. The core level difference $\Delta E_{\text{C},\text{C}'}$ between the two Cd compounds is obtained from the calculation for the $(\text{CdX})_n/(\text{CdY})_n$ superlattices with (001) orientation. The superlattice layer thickness n is increased until the core levels of the innermost layer on each side of the superlattice are bulk-like. The small orientational dependence and strain dependence of the core levels¹⁹ are neglected. The uncertainty in the calculated valence band offset is about 0.05 eV. A compilation of predicted valence band offsets of all II-VI and III-V systems is given in Ref. 8.

The method of Eq. (1) necessitates not only calculation of bulk CdX and CdY, but also the CdX/CdY heterojunction. In this sense, it is more accurate than the ‘‘model solid’’ method of Van de Walle²⁰ or the ‘‘dielectric midgap level’’ approach of Cardona and Christensen²¹ in that these methods all *assume* level lineup from calculations of isolated binary compounds. On the other hand, our method is similar to pseudopotential approach²² where the core level energies in Eq. (1) are replaced by average potentials of the compounds on each side of the heterojunction.

B. Band gap bowing of random alloys

The band gaps $E_g(x)$ of random $\text{CdX}_{1-x}\text{Y}_x$ alloys are conventionally fitted to a bowing formula²³

$$E_g(x) = (1-x)E_g(\text{CdX}) + xE_g(\text{CdY}) - bx(1-x), \quad (2)$$

where b is the ‘‘optical bowing coefficient,’’ $E_g(x)$ is the band gap of the alloy at composition x , and $E_g(\text{CdX})$ and $E_g(\text{CdY})$ are the band gap of the binary constituents. To mimic the random alloy $\text{CdX}_{1-x}\text{Y}_x$, we use the ‘‘special quasirandom structures’’ (SQS)²⁴ approach, where one occupies the anion sites in a relatively small periodic unit cell by X and Y atoms so that the physically most relevant atom-atom correlation functions are forced to be closest to the exact values of a random alloy. This approach is more accurate than virtual crystal approximation²⁵ (VCA) which neglects the chemical identity of each atom by assuming averaged type of atom $\langle XY \rangle$ or the coherent potential approximation²⁶ (CPA) which assumes that each X (or Y)

atom has identical environment in the alloy. In the atomistic SQS approach both charge transfer and atomic displacements are included. The equilibrium atomic displacements of the $\text{CdX}_{1-x}\text{Y}_x$ are relaxed using the valence force field (VFF) model.^{27,28} We assume that the lattice constant follow the Vegard’s rule.²⁹ The LDA underestimate the band gaps. The calculated LDA band gaps are 0.85, 0.23, and 0.22 eV for CdS, CdSe, and CdTe, respectively, while the experimental band gaps at low temperature^{17,30} are 2.50, 1.76, and 1.61 eV, respectively. However, the effect of LDA error on the bowing parameter b in Eq. (2) is small since we are comparing chemically identical systems in two different forms: the $(\text{CdX})_{1-x}(\text{CdY})_x$ alloys versus equivalent amounts of the constituents CdX and CdY.

C. Formation energies and transition energy levels of defects

Defect calculations are performed by placing the point defect at a center of an artificially large unit cell containing 64 atoms. We then impose periodic boundary conditions on this ‘‘supercell’’ so that the Schrodinger equation for this system can be solved using standard band structure methods. Atoms are displaced until the quantum-mechanical forces vanish, thus yielding the equilibrium geometry. At this point, we compute the total energy $E(\alpha, q)$ and energy levels for a cell containing the relaxed defect α in charge state q . The charge state is determined by the number of electrons we add to or remove from the gap levels. We also compute the total energy $E(\text{CdX})$ for the same supercell in the absence of the defect. From these quantities we deduce the ‘‘defect formation energy’’ $\Delta H_f(\alpha, q)$. It depends on⁹ the Fermi energy ϵ_F as well as on the atomic chemical potentials μ_i . The reason that ΔH_f depends on the chemical potentials is that in forming a defect such as vacancy, the removed atom is transferred to a ‘‘chemical reservoir’’ that has a characteristic energy called the chemical potential μ_i . Similarly, the reason that ΔH_f depends on the Fermi energy is that in forming a charged defect, electron is transferred to or from an electron reservoir whose energy is ϵ_F . In CdX:

$$\Delta H_f(\alpha, q) = \Delta E(\alpha, q) + n_{\text{Cd}}\mu_{\text{Cd}} + n_{\text{X}}\mu_{\text{X}} + n_{\text{A}}\mu_{\text{A}} + q\epsilon_F, \quad (3)$$

where

$$\Delta E(\alpha, q) = E(\alpha, q) - E(\text{CdX}) + n_{\text{Cd}}\mu_{\text{Cd}}^0 + n_{\text{X}}\mu_{\text{X}}^0 + n_{\text{A}}\mu_{\text{A}}^0 + qE_V. \quad (4)$$

Here, $\epsilon_F = \epsilon_F^a - E_V$ (‘‘a’’ denotes absolute values) is the Fermi energy of the electrons referenced to the valence band maximum (VBM) of CdX. $\mu_i = \mu_i^a - \mu_i^0$ is the chemical potential of constituent i relative to its chemical potential μ_i^0 in the stable phase (elemental solids). The n ’s are the numbers of Cd, anion X, and extrinsic defect A, and q is the number of electrons, transferred from the supercell to the reservoir in forming the defect cell. [E.g., for the $\text{Cu}_{\text{Cd}}^{-1}$ defect, $n_{\text{Cu}} = -1$, $n_{\text{Cd}} = 1$, $q = -1$, and others are null.] The value of $\Delta H_f(\alpha, q)$ tells us how much energy it takes to form defect α in charge state q for a given level of doping (thus, given ϵ_F) and given stoichiometry (i.e., the chemical potential which determines whether it is Cd or X rich).

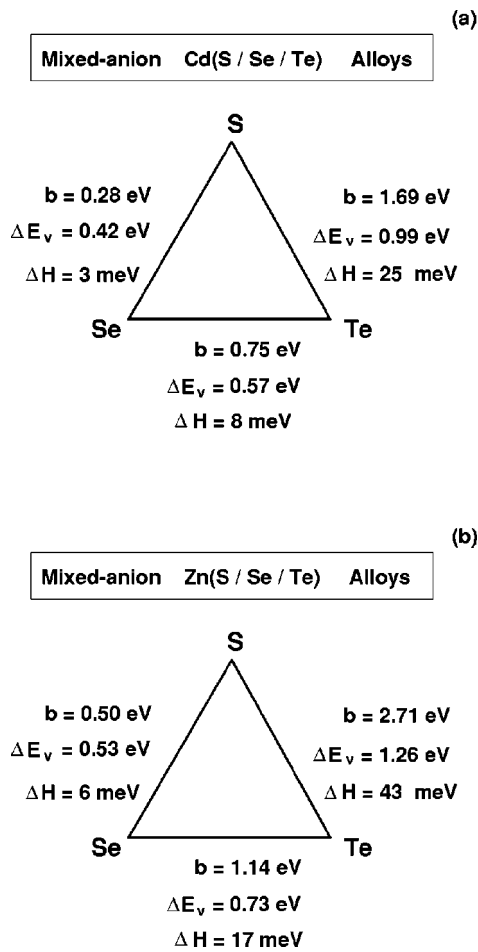


FIG. 1. Calculated bowing coefficients b , valence band offsets ΔE_v , and alloy mixing energies ΔH at $x=1/2$ of Cd-based alloys. ΔH is given in meV per atom. Results for Zn-based alloys are also included for comparison.

The “defect transition energy level” $\epsilon_\alpha(q/q')$ is the Fermi energy ϵ_F in Eq. (3) at which the formation energy $\Delta H_f(\alpha, q)$ of defect α of charge q is equal to that of another charge q' of the same defect, i.e.,

$$\epsilon_\alpha(q/q') = [\Delta E(\alpha, q) - \Delta E(\alpha, q')] / (q' - q). \quad (5)$$

For example, $\epsilon_\alpha(-/0)$ is an acceptor level. When ϵ_F is below $\epsilon_\alpha(-/0)$ the defect α is neutral, while defect α is negatively charged when ϵ_F is above $\epsilon_\alpha(-/0)$. $\epsilon_\alpha(q/q')$ tells us where in the gap can we find the donor and acceptor levels of defect α .

Due to the small cell-size and small basis set used in the present calculation we estimate that the error in the calculated formation energies is about 0.2 eV and the error in the calculated transition energies is about 0.1 eV. LDA error in the band gap error further introduce uncertainties in the calculated results, especially for the deep levels.

III. RESULTS

Figure 1 summarizes ΔH , b , and ΔE_v for CdS, CdSe, and CdTe. For comparison, we repeat the corresponding values³¹ for ZnS, ZnSe, and ZnTe in Fig. 1b. We next discuss the salient features in Fig. 1.

A. Mixing enthalpies

The mixing enthalpy of the random $\text{CdX}_x\text{Y}_{1-x}$ alloy at $x=0.5$ can be obtained from the calculated alloy total energies as

$$\Delta H(x=1/2) = E_{\text{tot}}(\text{CdX}_{0.5}\text{Y}_{0.5}) - \frac{1}{2}E_{\text{tot}}(\text{CdX}) - \frac{1}{2}E_{\text{tot}}(\text{CdY}). \quad (6)$$

Our calculated values (in meV/atom) are denoted as ΔH in Fig. 1(a). We find the following results:

(i) The mixing enthalpies are all positive and increases as the lattice mismatch between the constituents increases. For example, $\Delta H(\text{CdS}_{0.5}\text{Se}_{0.5})$, $\Delta H(\text{CdSe}_{0.5}\text{Te}_{0.5})$, and $\Delta H(\text{CdS}_{0.5}\text{Te}_{0.5})$ are 3, 8, and 25 meV/atom, respectively, and the corresponding size-mismatches $\Delta a/\bar{a}$ are 3.8%, 6.9%, and 10.7%, respectively. (For Zn alloys, the corresponding lattice mismatch are 4.6%, 7.2%, and 11.8%, respectively). The positive sign of ΔH indicates that the ground state of these alloys at $T=0$ corresponds to phase separation into the binary zinc-blende constituents. However, at finite temperatures, the disordered phase can be stabilized through entropy. The mixing enthalpy ΔH is rather small for $\text{CdS}_x\text{Se}_{1-x}$ alloy, suggesting that $\text{CdS}_x\text{Se}_{1-x}$ will be miscible in the whole composition range at finite temperatures. The mixing enthalpy ΔH is large for the $\text{CdS}_x\text{Te}_{1-x}$ alloy, suggesting that large miscibility gap exist in $\text{CdS}_x\text{Te}_{1-x}$ [e.g., using the regular solution model, where the free energy F is given by $F = \Omega x(1-x) + kT\{x \ln x + (1-x) \ln(1-x)\}$ and $\Omega = 4\Delta H(x=0.5)$, we estimate that the miscibility is about 8% at $T=800$ K].

(ii) Cd alloys have smaller mixing enthalpies than the corresponding Zn alloys. This is mainly due to the smaller lattice mismatch and smaller bulk moduli¹⁸ of the Cd alloys (thus, smaller elastic strain energies) relative to the Zn alloys.

B. Band offsets

Using the procedure described in Sec. II A we have calculated the unstrained natural valence band offsets between the cubic II-VI CdS/CdSe/CdTe compounds (Fig. 2). The conduction band offsets ΔE_c are obtained using the relation

$$\Delta E_c = \Delta E_g + \Delta E_v, \quad (7)$$

where ΔE_g is the measured^{17,30} band gap differences between the compounds. We find the following results:

(i) The S/Se unstrained band lineup is “type I,” while the S/Te and Se/Te band lineup is “type II.”

(ii) The band offsets are large in the valence band, but small in the conduction band. The large valence band offsets for this mixed anion system are consistent with the fact that the VBM is anion p -like state, and that the anion p orbital energies increase significantly as anion atomic number increases (Table I). The small conduction band offsets are also consistent with the fact that CBM is mostly cation s states with only minor contributions from anion s orbitals. It is interesting to see that the order of the CBM in CdX follow the same trend as the anion X s atomic orbital energies (Table I).

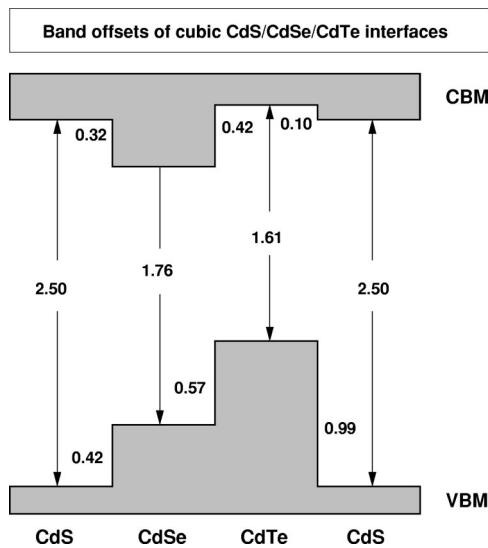


FIG. 2. Calculated natural valence band and conduction band offsets for interfaces between Cd-based compounds.

(iii) The valence band offsets between the Cd compounds are smaller than those between the corresponding Zn compounds (Fig. 1). The reason⁷ is as follows: In the zincblende compound with T_d site symmetry both the anion p and the cation d orbitals transform (among others) as the Γ_{15} (also called t_2) representation. These two equal-symmetry states interact with each other, in direct proportion to the $p-d$ coupling matrix element and in inverse proportion to the energy difference $\epsilon_p^{\text{anion}} - \epsilon_d^{\text{cation}}$. The interaction between the anion p and the occupied cation d states results in a level repulsion, moving the VBM upwards.⁷ This $p-d$ coupling tends to reduce the valence band offsets.⁸ This is so since the S p orbital is deeper (i.e., closer to the metal d orbital) than the Se p or Te p (Table I) and it has a smaller size than Se or Te, so S p couples more to cation d than Se p or Te p do. Consequently, the VBM of sulphides moves up more than the VBM of selenides or tellurides, thus reducing the band offsets between sulphides and selenides or tellurides. We find that this effect of reduction of valence band offset by $p-d$ coupling is weaker in Zn compounds ZnX/ZnY than in CdX/CdY. This is so because the Zn $3d$ orbitals are more localized than the Cd $4d$ orbitals.

(iii) The natural band offsets given in Fig. 1 are calculated for relaxed unstrained interface where the compounds on either sides of the interface take their respective equilibrium lattice constant values. If on the other hand the compounds are coherently strained to a substrate, the band offsets will depend on the substrate lattice constant a_s . For ex-

TABLE I. Calculated (semirelativistic) atomic LDA valence orbital energies ϵ_s , ϵ_p , and ϵ_d (in eV) of the elements studied in this article.

Atom	ϵ_s	ϵ_p	ϵ_d
S	-17.36	-7.19	
Se	-17.56	-6.74	
Te	-15.43	-6.19	
Cd	-6.04	-1.41	-11.96
Zn	-6.31	-1.31	-10.49

ample, for CdS/CdTe, the natural unstrained band offset is 0.99 eV, while the calculated band offsets between the highest valence state strained on CdS, CdS_{0.5}Te_{0.5}, and CdTe are 1.54, 1.10, and 0.80 eV, respectively.

Niles and Hochst³² measured the valence band offset for CdS/CdTe using the photoemission method. Their measured value of $\Delta E_v = 0.65$ eV is smaller than our calculated value of 0.99 eV and will lead to a type-I band alignment between CdS and CdTe, while our calculated results suggest that it should be type-II. Further studies are needed to solve this discrepancy.

C. Optical bowing coefficients in random alloys

The optical bowing parameter b of the alloy is given by

$$b = [E_g(\text{CdX}_{1-x}\text{Y}_x) - (1-x)E_g(\text{CdX}) - xE_g(\text{CdY})] / [x(1-x)]. \quad (8)$$

Figure 1 gives the calculated bowing parameter for mixed-anion Cd alloys at $x=0.5$. We find the following results:

(i) The bowing coefficients have the following trend

$$b(\text{S,Se}) < b(\text{Se,Te}) < b(\text{S,Te}). \quad (9)$$

This trend is consistent with the observation^{23,24,33,34} that the bowing parameters increases with chemical and size disparity of the constituents. For the system studied here, Cd(S,Se) has a rather small bowing ($b=0.28$ eV), since the lattice mismatch between CdS and CdSe is small and the s atomic eigenvalue difference (~ 0.20 eV) and the p atomic eigenvalue difference (~ 0.45 eV) between S and Se are relatively small (Table I). On the other hand, the lattice mismatch between CdS and CdTe is large and the s atomic eigenvalue difference (~ 1.93 eV) and the p atomic eigenvalue difference (~ 1.00 eV) between S and Te are large, so the bowing coefficient for Cd(S,Te) is large.

The measured optical bowing parameter for CdS_{1-x}Te_x are 1.74 (Ref. 35), 1.70 (Ref. 36), and 1.84 eV (Ref. 37), assuming Eq. (2). These results are in good agreement with our calculated value of $b=1.69$ eV at $x=0.5$. However, it is also clear from the experimental data³⁷ that bowing parameter in the S rich limit is considerably larger than the one at $x=0.5$ (see below).

The measured band gap as a function of composition using optical absorption³⁸ and reflectance³⁹ methods for *thin-film* CdS_{1-x}Se_x alloy show that the band gap has a *negative* bowing parameter, in contradiction to our calculations ($b=0.28$ eV) and early experimental results^{40,41} for bulk alloy ($b=0.31$ eV). The discrepancy may be due to the difficulty in determining the alloy composition of the chemical bath deposited thin-film samples, and phase transition and amorphous structure observed in these samples.

For CdSe_{1-x}Te_x the measured bowing parameter $b \sim 0.8$ eV for bulk alloy⁴² is in good agreement with our calculated value of $b=0.75$ eV.

(ii) The bowing coefficients for the CdX_{1-x}Y_x alloys are smaller than the corresponding Zn alloys (Fig. 1). This correlates with the fact that CdX/CdY valence band offsets and the lattice mismatch are smaller than ZnX/ZnY. The small

size mismatch and chemical disparity in VBM in Cd compounds lead to a smaller bowing in Cd alloys than in the Zn alloys.

(iii) For most semiconductor alloys the bowing coefficient b is nearly independent of composition x .^{17,43} However, for alloys with large size and chemical disparity between its constituents, the bowing coefficient could be strongly composition dependent.⁴⁴ We find that this is the case for S/Te alloy. The bowing coefficient b for $\text{CdS}_{1-x}\text{Te}_x$, to a good approximation, can be described as

$$b(x) = 3.90 - 6.93x + 5.01x^2. \quad (10)$$

The large bowing coefficient at the Te dilute limit ($b \sim 3.9$ eV) can be traced to strong VBM wave function localization on Te site with higher p orbital energy. In fact, in the impurity limit Te substitution on S site lead to a localized isovalent impurity level (see below). This result indicates that even a small amount of Te in CdS can drastically reduce its band gap.³⁷ It is also interesting to notice that in the S dilute limit, the CBM is weakly localized on the S site which has low s orbital energy (Table I). This weak localization is responsible to the increased bowing ($b \sim 2.0$ eV) in the S dilute limit.

(iv) One of the methods to increase the open-circuit voltage V_{oc} , thus the efficiency in CdTe-based solar cell, is to increase its band gap. It has been suggested⁴⁵ that this can be achieved by alloying CdTe with a large gap material such as CdSe or CdS. This can also reduce the interface strain between CdTe absorber and the CdS window. However, addition of small amounts of a large-gap material B into a small-gap material A does not always raise the gap of the latter. This is clear from Eq. (2) which show that

$$dE_g/dx|_{x=0} = [E_g(B) - E_g(A)] - b. \quad (11)$$

This means that at low x the band gap increases with x only if the band gap difference $[E_g(B) - E_g(A)]$ is larger than the bowing parameter b . Our calculations show that for both $\text{CdTe}_{1-x}\text{Se}_x$ and $\text{CdTe}_{1-x}\text{S}_x$ alloys the bowing coefficient is larger than the band gap difference of the constituents, indicating that initially, addition of S and Se into CdTe will actually reduce the band gap, instead of increasing it. Further increase of S or Se concentration will eventually increase the band gap, but this will also reduce the quality of the alloy due to the large miscibility gap and the poor p -type dopability of CdS and CdSe. We believe that adding ZnTe to CdTe is a better choice for opening the band gap of the latter, since the optical bowing parameter of $\text{Cd}_{1-x}\text{Zn}_x\text{Te}$ alloy ($b = 0.23$ eV)⁴⁶ is smaller than the band gap differences $E_g(\text{ZnTe}) - E_g(\text{CdTe}) = 0.8$ eV.¹⁷ Thus, addition of ZnTe will increase the gap of CdTe while addition of CdSe or CdS will reduce it. The valence band offset between CdTe and ZnTe (~ 0.09 eV)⁸ is also small, thus the two compounds and their alloys are expected to have similar p -type dopabilities.^{9,47}

D. The isovalent defect CdS:Te

In conventional isovalent semiconductor alloys such as $\text{GaP}_{1-x}\text{As}_x$, the electronic properties vary smoothly with composition.⁴⁸ In these alloys the band edges shift as a

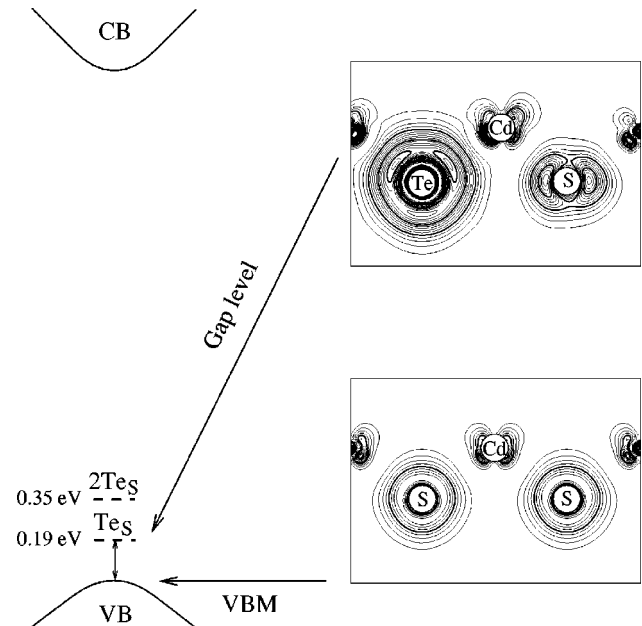


FIG. 3. Calculated defect levels of a single Te impurity and nearest neighbor Te-Te defect pairs in CdS. The electronic charge density plots compares the charge distribution of the Te_S defect level with that of ideal CdS VBM.

whole as the alloy composition increases. This reflects the fact that most isovalent impurities do not induce defect energy levels in the band gap. However, when the two constituents of the alloy have a large difference in their atomic potentials and atomic sizes, localized isovalent defect states can exist inside the band gap, leading to abrupt changes in the alloy optical properties.⁴⁹ These isovalent defect levels have been observed in mixed anion systems, e.g., in GaN:P ,⁵⁰ ZnS:Te ,⁵¹ and CdS:Te .⁵¹⁻⁵⁴ For CdS:Te these isovalent defect levels act as isoelectronic traps which are able to bind an exciton.⁵ Thus, even a small amount of Te in CdS could have significant detrimental effects on its device applications. We have calculated the defect energy levels of Te impurity and nearest neighbor Te impurity pairs in CdS. The calculated energy levels and charge density distributions of the gap levels are plotted in Fig. 3. We find the following results:

(i) For single substitutional Te impurity in CdS, the symmetry around the impurity site is T_d . The calculated position of the t_2 single-particle defect level is at $E_v + 0.19$ eV. With spin-orbit coupling, this state is fourfold degenerate and consists mostly of anion p orbitals. Figure 3 shows that the wave function of the defect state is primarily localized on the impurity site. Similar results are obtained for single substitutional Te impurity in ZnS, where the single particle defect energy level is calculated to be at $E_v + 0.29$ eV.

(ii) If two Te atoms replace face-centered-cubic (fcc) nearest-neighbor S sites in CdS, the symmetry is reduced to C_{2v} . The highest defect state is doubly degenerate with single particle defect level at $E_v + 0.35$ eV. The Te-Te impurity pair binding energy, i.e., the energy of the nearest neighbor Te-Te pair relative to the energy of two isolated Te impurity, is found to be -7 meV/pair, indicating that at $T = 0$ the formation of Te-Te impurity pair is favored.

TABLE II. Defect formation energies in term of $\Delta E(\alpha, q)$ in Eq. (4) and defect transition levels $\epsilon_{\alpha}(q/q')$ of Eq. (5) in CdS and CdTe. The n_{Cu} and n_{Cd} are the numbers of Cu and Cd atoms and q is the number of excess electrons, transferred from the defect-free crystal to the reservoirs to form one defect.

Defect α	$\Delta E(\alpha, q)$ (eV)	n_{Cu}	n_{Cd}	q
CdS				
Cu_{Cd}^0	1.70			0
Cu_{Cd}^-	2.34	-1	+1	-1
Defect transition level:	$(-/0)=E_V+0.64$ eV			
V_{Cd}^0	4.10			0
V_{Cd}^-	4.43	0	+1	-1
V_{Cd}^{2-}	4.94			-2
Defect transition levels:	$(-/0)=E_V+0.33$ eV; $(2-/ -)E_V+0.51$ eV;			
CdTe				
Cu_{Cd}^0	1.01			0
Cu_{Cd}^-	1.15	-1	+1	-1
Defect transition level:	$(-/0)=E_V+0.14$ eV			
V_{Cd}^0	2.30			0
V_{Cd}^-	2.42	0	+1	-1
V_{Cd}^{2-}	2.69			-2
Defect transition levels:	$(-/0)=E_V+0.12$ eV; $(2-/ -)E_V+0.27$ eV;			

The calculated (+/0) transition energy levels is at $E_V + 0.18$ eV for isolated CdS:Te impurity. The donor level (+/0) is at $E_V + 0.42$ eV for Te-Te nearest neighbor impurity pairs. These results can be compared with experimental data of 0.22 and 0.44 eV, respectively, derived from photoluminescence measurements.⁵¹⁻⁵⁴ We see that the general agreement is good. The smaller calculated values relative to the measured values could be caused by the LDA error in the band gap.

E. Defect formation energies and defect transition energy levels

CdTe is the only II-VI compound which can be doped relatively easily either *p* or *n* type.⁵⁵ Many of the devices, e.g., solar cells use *p*-type CdTe as absorber.^{1,2} Beside defect pairs such as the A center,⁵⁶ the leading candidates of the *p*-type dopant in CdTe is Cd vacancy V_{Cd} and Cu substitution on Cd sites Cu_{Cd} . Using the method described in Sec. II C, we have calculated the formation energies and transition energy levels of these two cation point defects. Results are shown in Table II. Figure 4 shows $\Delta H_f(Cu_{Cd}^q)$ as a function of Fermi energy for $q=0$ and $q=-1$ in CdS (solid lines) and CdTe (dashed lines) for $\mu=0$. The lines for $q=0$ in CdS and CdTe are horizontal since $\Delta H_f(Cu_{Cd}^{q=0})$ is independent of ϵ_F [Eq. (4)], while $\Delta H_f(Cu_{Cd}^{q=-1})$ decreases as ϵ_F increases. At a critical energy $\epsilon_F = \epsilon_{pin}^{(n)}$ (shaded dots) the formation energy becomes zero, indicating that $Cu_{Cd}^{q=-1}$ will form spontaneously, thus will compensate donors and limit the *n*-type doping. Figure 5 shows similar results for V_{Cd}^q . We find the following results:

(i) Cu_{Cd} formation energy: For neutral Cu_{Cd}^0 defect the calculated defect formation energy at $\mu_i=0$ is 1.70 eV for CdS and 1.01 eV for CdTe. For the negatively charged defect Cu_{Cd}^- , it is 2.34 eV for CdS and 1.15 eV for CdTe when

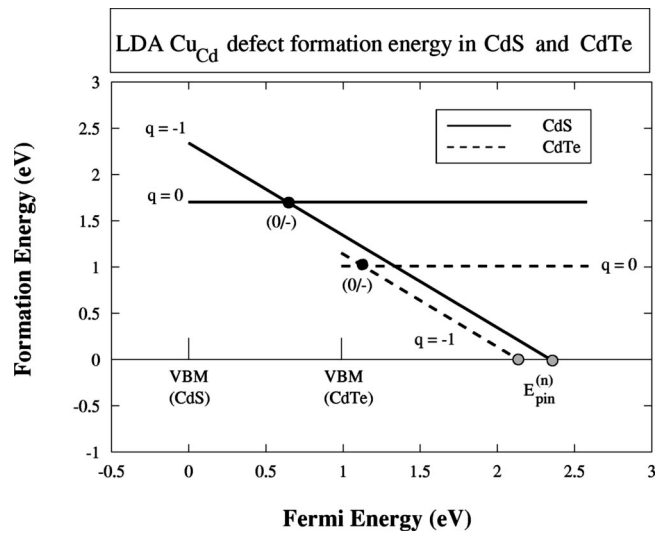


FIG. 4. LDA calculated $\Delta H_f(Cu_{Cd}^q)$ as a function of Fermi energy in CdS (solid lines) and CdTe (dashed lines) for $\mu = \mu_{solid}$. The solid dots show the electrical transition energy levels and the shaded dots show the position of the pinning energy $\epsilon_{pin}^{(n)}$ of the closed-shell defect Cu_{Cd}^- .

the Fermi energy is taken at their respective VBMs (Fig. 4). If we use a common Fermi energy, e.g., $E_F = E_{VBM}(CdS) + 0.99$ eV = $E_{VBM}(CdTe)$, the formation energy of Cu_{Cd}^- in CdS is reduced to 1.35 eV, similar to the 1.15 eV found in CdTe (Fig. 4). Notice that in an *n*-CdS/*p*-CdTe heterojunction, the Fermi energy on CdS side is close to its CBM and on the CdTe side is close to its VBM, thus the formation energy of Cu_{Cd}^- could be lower in *n*-CdS than in *p*-CdTe,

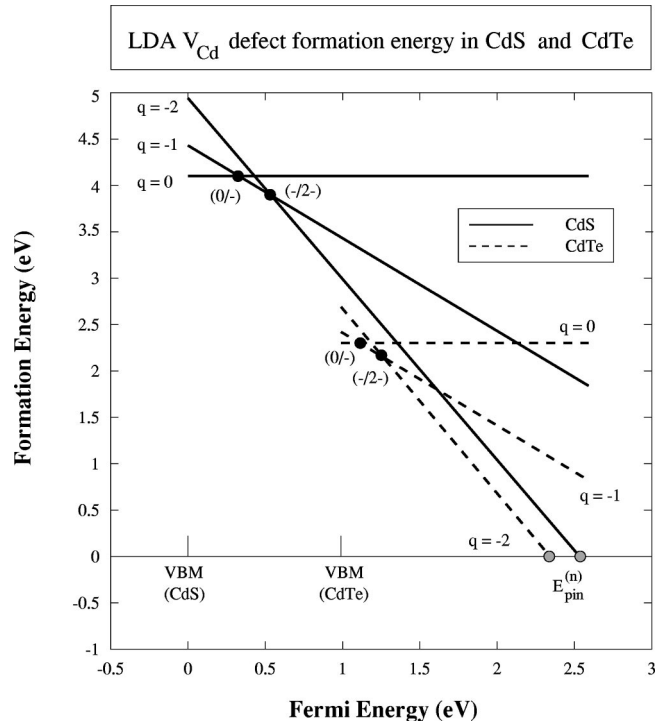


FIG. 5. LDA calculated $\Delta H_f(V_{Cd}^q)$ as a function of Fermi energy in CdS (solid lines) and CdTe (dashed lines) for $\mu = \mu_{solid}$. The solid dots show the electrical transition energy levels and the shaded dots show the position of the pinning energy $\epsilon_{pin}^{(n)}$ of the closed-shell defect V_{Cd}^{2-} .

leading to a diffusion of Cu atom from the p -CdTe layer to the n -CdS layer. This type of Cu diffusion has been observed experimentally in CdS/CdTe solar cells.⁵⁷

(ii) V_{Cd} formation energy: For neutral V_{Cd}^0 defect the calculated defect formation energy at $\mu_{Cd}=0$ is 4.10 eV for CdS and 2.30 eV for CdTe. For the singly negatively charged defect V_{Cd}^- , ΔH is 4.43 eV for CdS and 2.42 eV for CdTe; and for the doubly negatively charged defect V_{Cd}^{2-} , it is 4.94 eV for CdS and 2.69 eV for CdTe, if the Fermi energy is taken at their respective VBM (Fig. 5). Again, we find that if we use a common Fermi energy in an absolute energy scale, and let $E_F = E_{VBM}(CdS) + 0.99$ eV $= E_{VBM}(CdTe)$, the formation energy of the closed shell defect V_{Cd}^{2-} in CdS is 2.96 eV, similar to the 2.69 eV found in CdTe. The fact that, using an absolute energy scale for the Fermi energy, the formation energies of certain closed shell defects (e.g., Cu_{Cd}^- and V_{Cd}^{2-}) are similar in a class of material (e.g., CdX) [thus, similar $\epsilon_{pin}^{(n)}$] has also been found in another system.¹⁰ This phenomena has been described in Ref. 10 and is used to explain the phenomenological “doping limit rule” in semiconductors and insulators.

(iii) Since the formation energies of Cu_{Cd} is smaller than V_{Cd} , presence of Cu in the sample is expected to eliminate the V_{Cd} defect. To aid the search of the Cu_{Cd} substitutional defect we have calculated the Cu-X bond length in CdX compounds. We find that the Cu-X bond lengths are about 6.7% smaller than the Cd-X bond lengths.

(iv) Cu_{Cd} transition energy levels: The calculated Cu_{Cd} (0/-) transition energy levels is $E_{VBM} + 0.64$ eV for CdS and $E_{VBM} + 0.14$ eV for CdTe (solid dots in Fig. 4). This indicates that Cu_{Cd} creates a shallow acceptor level in CdTe, thus Cu doping in CdTe produces good conductivity. But Cu_{Cd} creates deep acceptor levels in CdS, and thus will not produce low conductivity samples. However, because the transition energy level difference $0.64 - 0.14 = 0.50$ eV is smaller than the valence band offset between CdS and CdTe (0.99 eV), in an absolute energy scale, the two transition energy levels do not line up. This indicates that the “vacuum pinning rule,”¹¹ which suggests that in a class of material (e.g., II-VI) deep levels line up in an absolute energy scale, is not followed exactly in this case. This is partly due to the fact that Cu_{Cd} is not a very localized defect in CdX.

(v) V_{Cd} transition energy levels: The calculated V_{Cd} (0/-) transition energy levels is $E_{VBM} + 0.33$ eV in CdS and $E_{VBM} + 0.12$ eV in CdTe. For the (-/-) transition the calculated energy levels is $E_{VBM} + 0.51$ eV in CdS and $E_{VBM} + 0.27$ eV in CdTe (solid dots in Fig. 5). Again the acceptor levels are deep in CdS than in CdTe. These deep levels in CdS will act as electronic trap, thus photogenerated holes in CdS will not contribute to the photocurrent.

Using electron paramagnetic resonance method Emanuelsson *et al.*⁵⁸ found that in CdTe the V_{Cd} (-/-) transition energy level is located at a position less than $E_V + 0.47$ eV. Using admittance spectroscopy Reislochner *et al.*⁵⁹ found that it is located at $E_V + 0.23$ eV. These values are in good agreement with our calculated value at $E_V + 0.27$ eV.

IV. SUMMARY

In summary, we have studied systematically the electronic properties of Cd-based compounds, alloys, interfaces, and Cu_{Cd} and V_{Cd} impurities using the first-principles, self-consistent electronic structure theory based on the local density approximation (LDA). We find that (i) the mixing enthalpies are all positive and increases as the lattice mismatch between the constituents increases. A large miscibility gap exist in CdS_xTe_{1-x} . (ii) The S/Se band lineup is type I, while the S/Te and Se/Te band lineup is type II. The band offsets are large in the valence band, but small in the conduction band. (iii) The bowing coefficients have the following trend $b(S,Se) < b(Se,Te) < b(S,Te)$. For CdS_xTe_{1-x} we also find that the bowing coefficient b depends strongly on x . (iv) Substitutional Te impurities in CdS form isovalent defect levels inside the band gap. These isovalent defects form electron traps and are responsible for large band gap reduction and low photocurrent in the CdS layer (leading to lower quantum efficiency) when only a small amount of Te is present in CdS. (v) Cu_{Cd} and V_{Cd} create shallow acceptor levels in CdTe, but the levels are much deeper in CdS, thus, one cannot produce low conductivity samples in p -CdS. (vi) The formation energies of closed shell defects (Cu_{Cd}^- and V_{Cd}^{2-}) are similar in CdS and CdTe, thus, supporting the explanation of the phenomenological “doping limit rule.”

ACKNOWLEDGMENTS

We thank D. Albin, R. G. Dhere, D. H. Levi, P. Sheldon, and X. Z. Wu for helpful discussions. This work was supported in part by U.S. Department of Energy, Grant No. DE-AC36-98-GO10337.

- ¹R. W. Birkmire and E. Eser, *Annu. Rev. Mater. Sci.* **27**, 625 (1997).
- ²A. D. Compaan, J. R. Sites, R. W. Birkmire, C. S. Ferekides, and A. L. Fahrenbruch, in *Proceedings of Workshop of Basic Research Opportunities in Photovoltaics*, 1999 (unpublished).
- ³J. Britt and C. Ferekides, *Appl. Phys. Lett.* **62**, 2851 (1993).
- ⁴D. G. Jensen, B. E. McCandless, and R. W. Birkmire, in *Proceedings of the 25th PVSC Conference* (IEEE, New York, 1996), p. 773.
- ⁵D. H. Levi, B. D. Fluegel, R. K. Ahrenkiel, A. D. Compaan, and L. M. Woods, in *Proceedings of the 25th PVSC Conference* (IEEE, New York, 1996), p. 913.
- ⁶A. Rohatgi, S. A. Ringel, R. Sudharsanan, and H. C. Chou, in *Proceedings of the 22nd PVSC Conference* (IEEE, New York, 1991), p. 962.
- ⁷S.-H. Wei and A. Zunger, *Phys. Rev. Lett.* **59**, 144 (1987); *Phys. Rev. B* **37**, 8958 (1988).
- ⁸S.-H. Wei and A. Zunger, *Appl. Phys. Lett.* **72**, 2011 (1998).
- ⁹S. B. Zhang, S.-H. Wei, and A. Zunger, *J. Appl. Phys.* **83**, 3192 (1998).
- ¹⁰S. B. Zhang, S.-H. Wei, and A. Zunger, *Phys. Rev. Lett.* (in press).
- ¹¹M. Caldas, A. Fazzio, and A. Zunger, *Appl. Phys. Lett.* **45**, 671 (1984).
- ¹²P. Hohenberg and W. Kohn, *Phys. Rev.* **136**, B864 (1964); W. Kohn and L. S. Sham, *ibid.* **140**, A1133 (1965).
- ¹³S.-H. Wei and H. Krakauer, *Phys. Rev. Lett.* **55**, 1200 (1985), and references therein.
- ¹⁴D. M. Ceperly and B. J. Alder, *Phys. Rev. Lett.* **45**, 566 (1980).
- ¹⁵J. P. Perdew and A. Zunger, *Phys. Rev. B* **23**, 5048 (1981).
- ¹⁶S. Froyen, *Phys. Rev. B* **39**, 3168 (1989).
- ¹⁷*Semiconductors: Basic Data*, 2nd ed., edited by O. Madelung (Springer, Berlin, 1982).
- ¹⁸S.-H. Wei and A. Zunger, *Phys. Rev. B* **60**, 5404 (1999).
- ¹⁹A. Franceschetti, S.-H. Wei, and A. Zunger, *Phys. Rev. B* **50**, 17797 (1994).
- ²⁰C. G. Van de Walle, *Phys. Rev. B* **39**, 1871 (1989).
- ²¹M. Cardona and N. E. Christensen, *Phys. Rev. B* **35**, 6182 (1987).

- ²²R. G. Dandrea, C. B. Duke, and A. Zunger, *J. Vac. Sci. Technol. B* **10**, 1744 (1992).
- ²³J. E. Bernard and A. Zunger, *Phys. Rev. B* **36**, 3199 (1987).
- ²⁴A. Zunger, S.-H. Wei, L. G. Ferreira, and J. E. Bernard, *Phys. Rev. Lett.* **65**, 353 (1990); S.-H. Wei, L. G. Ferreira, J. E. Bernard, and A. Zunger, *Phys. Rev. B* **42**, 9622 (1990).
- ²⁵L. Nordheim, *Ann. Phys. (Leipzig)* **9**, 607 (1931).
- ²⁶B. Velicky, S. Kirkpatrick, and H. Ehrenreich, *Phys. Rev.* **175**, 747 (1968).
- ²⁷P. N. Keating, *Phys. Rev.* **145**, 637 (1996).
- ²⁸J. L. Martins and A. Zunger, *Phys. Rev. B* **30**, 6217 (1987).
- ²⁹L. Vegard, *Z. Phys.* **5**, 17 (1921).
- ³⁰We derive the band gap of zinc-blende CdSe from the experimental band gap for wurtzite CdSe and LDA band gap difference between zinc-blende and wurtzite CdSe. See C.-Y. Yeh, S.-H. Wei, and A. Zunger, *Phys. Rev. B* **50**, 2715 (1994).
- ³¹S.-H. Wei and A. Zunger, *J. Appl. Phys.* **78**, 3846 (1995).
- ³²D. W. Niles and H. Hochst, *Phys. Rev. B* **41**, 12710 (1990).
- ³³S.-H. Wei and A. Zunger, *Phys. Rev. B* **43**, 1662 (1991); *ibid.* **43**, 14272 (1991).
- ³⁴S.-H. Wei and A. Zunger, *Phys. Rev. B* **39**, 3279 (1989).
- ³⁵K. Ohata, J. Saraie, and T. Tanaka, *Jpn. J. Appl. Phys.* **12**, 1641 (1973).
- ³⁶A. D. Compaan, Z. Feng, G. Contreras-Puente, C. Narayanswamy, and A. Fischer, *Mater. Res. Soc. Symp. Proc.* **426**, 367 (1996).
- ³⁷K. Wei, F. Pollak, J. L. Freeouf, D. Shvydka, and A. D. Compaan, *J. Appl. Phys.* **85**, 7418 (1999).
- ³⁸R. S. Mane and C. D. Lokhande, *Thin Solid Films* **304**, 56 (1997).
- ³⁹V. Kumar and T. P. Sharma, *J. Phys. Chem. Solids* **59**, 1321 (1998).
- ⁴⁰O. Goede, D. Hennig, and L. John, *Phys. Status Solidi B* **96**, 671 (1979).
- ⁴¹A. Naumov, S. Permogorov, A. Reznitsky, S. Verbin, and A. Klochikhin, *J. Cryst. Growth* **101**, 713 (1990).
- ⁴²M. S. Brodin, N. I. Vitrikhovskii, A. A. Kipen, and I. B. Mizetskaya, *Sov. Phys. Semicond.* **6**, 698 (1972); [*Fiz. Tekh. Poluprovodn.* **6**, 601 (1972)].
- ⁴³*Landolt-Bornstein: Numerical Data and Functional Relationships in Science and Technology*, edited by O. Madelung, M. Schulz, and H. Weiss, (Springer, Berlin, 1982), Vol. 17b.
- ⁴⁴S.-H. Wei and A. Zunger, *Phys. Rev. Lett.* **76**, 664 (1996); L. Bellaiche, S.-H. Wei, and A. Zunger, *Phys. Rev. B* **54**, 17568 (1996).
- ⁴⁵X. Z. Wu (private communication).
- ⁴⁶S.-H. Wei and A. Zunger, *Phys. Rev. B* **43**, 1662 (1991).
- ⁴⁷T. A. Gessert, X. Li, T. J. Coutts, A. R. Mason, and R. J. Matson, *J. Vac. Sci. Technol. A* **12**, 1501 (1994).
- ⁴⁸L. Bellaiche, S.-H. Wei, and A. Zunger, *Phys. Rev. B* **56**, 10233 (1997).
- ⁴⁹S. Permogorov and A. Reznitsky, *J. Lumin.* **52**, 201 (1992).
- ⁵⁰D. G. Thomas, J. J. Hopfield, and C. J. Frosch, *Phys. Rev. Lett.* **15**, 857 (1966).
- ⁵¹D. Henning, O. Goede, and W. Heimbrodt, *Phys. Status Solidi B* **113**, K163 (1982).
- ⁵²D. M. Roessler, *J. Appl. Phys.* **41**, 4589 (1970).
- ⁵³T. Fukushima and S. Shionoya, *Jpn. J. Appl. Phys.* **15**, 813 (1976).
- ⁵⁴K. P. Tchakpele and J. P. Albert, *Phys. Status Solidi B* **149**, 641 (1988).
- ⁵⁵R. G. Dhere, Ph.D. thesis, University of Colorado, 1997 (unpublished).
- ⁵⁶R. Krause-Rehberg, H. S. Leipner, T. Abgarjan, and A. Polity, *Appl. Phys. A* **66**, 599 (1998).
- ⁵⁷C. Narayanswamy, T. A. Gessert, and S. E. Asher, *AIP Conf. Proc.* **462**, 248 (1998).
- ⁵⁸P. Emanuelsson, P. Omling, B. K. Meyer, M. Wienecke, and M. Schenk, *Phys. Rev. B* **47**, 15578 (1993).
- ⁵⁹U. Reislochner, J. Grillenberger, and W. Witthuhn, *J. Cryst. Growth* **184/185**, 1160 (1998).